Detailed analysis of successive pTRMs carried by pyrrhotite in Himalayan metacarbonates: an example from Hidden Valley, Central Nepal.

Christian Crouzet, H. Stang, E. Appel, Eva Schill, P. Gautam

Geophys. J. Int. (2001) **146,** 607–618

Detailed analysis of successive pTRMs carried by pyrrhotite in Himalayan metacarbonates: an example from Hidden Valley, Central Nepal

C. Crouzet,[1] H. Stang,[1] E. Appel,[1] E. Schill[1] and P. Gautam[2]

[1] *Institut für Geologie und Paläontologie, Arbeitsbereich Geophysik, Universität Tübingen, Sigwartstrasse* 10, D-72076 *Tübingen, Germany. E-mails: christian.crouzet@uni-tuebingen.de; erwin.appel@uni-tuebingen.de*

[2] *Central Department of Geology, Tribhuvan University, Kirtipur, Kathmandu, Nepal*

Accepted 2001 April 2. Received 2001 March 2; in original form 2000 August 11

SUMMARY

Low-grade metacarbonates from the Tethyan Himalaya were sampled for palaeomagnetic studies in Hidden Valley (Central Nepal). The remanence is carried by pyrrhotite, evidenced by thermomagnetic runs of susceptibility (Hopkinson peak at $\sim 300\ ^{\circ}C$), alternating field demagnetization, isothermal remanent magnetization acquisition and subsequent thermal demagnetization. The palaeomagnetic directions reflect a Tertiary overprint after the main folding event, probably synchronous with the metamorphism. Normal and reverse remanence directions were separated and vary with altitude. It is also possible to retrieve several antiparallel components versus temperature during thermal demagnetization of a single sample. At higher altitudes (4920–5500 m), the first component recorded is reverse (R_1). At a lower temperature a normal component can be extracted (N_1). For sites sampled at lower altitudes (4700–4900 m), the high-temperature reverse component disappears but a medium-temperature reverse component (R_2) demagnetized in a narrow temperature range can be identified in between two normal components (N_1 at high temperature and N_2 at low temperature). At the lowest altitudes (4450–4700 m), only a normal component (N_2) appears. The occurrence of successive normal and reverse polarities in one sample is interpreted as the record of successive reversals of the geomagnetic field during the post-metamorphic Tertiary cooling of the studied area. The polarity versus altitude function is a powerful argument for a thermomagnetic origin of the magnetization. No obvious rotations around a vertical axis with respect to the stable Indian plate are evidenced for the Tertiary. However, the inclination is not consistent with the expected inclination. Main Central Thrust ramping can be invoked to explain our observations. R_1, N_1 and N_2 inclinations are slightly different and their tendency is consistent with tilting towards the north during magnetization acquisition. The minimum total amount of such tilting is around 25°. Accurate geochronological data from the Tethyan Himalaya would be of a great help for better resolution.

Key words: block rotation, chemical remanent magnetization, palaeomagnetism, partial thermoremanent magnetization, pyrrhotite, Tethyan Himalaya.

INTRODUCTION

The emerging recognition of the importance of magnetic overprinting occurring before, during or after deformation and sometimes also during metamorphism in sediments in mountains belts has led to the accumulation of a new type of palaeomagnetic data. Such data can be used for testing late block rotations or tectonic tilting. The major problem related to them, however, lies in the determination of the age and the nature of remagnetization. The debate on the nature of remagnetization has generally focused on two mechanisms: chemical and thermal remagnetization. Whatever the remagnetization process is, palaeomagnetic directions can be used to test block rotation. If the remagnetization is chemical, it is very difficult to obtain its age. In the case of a thermoremanent remagnetization, the cooling event corresponds to the time of remanence acquisition, and classical geochronological data could provide us with the age of the magnetization. Therefore, it is very important to find

out whether the remagnetization stems from chemical remanent magnetization (CRM) or from thermoremanent magnetization (TRM).

Secondary magnetizations are common in sedimentary rocks and several mechanisms have been invoked to explain these as a CRM (Elmore & McCabe 1991; Elmore *et al.* 1993; Katz *et al.* 2000). As a correlation between synfolding CRM and orogenic belts seems to exist, the role of orogenic fluids expelled during tectonic events has been one of the most commonly invoked possibilities for remagnetization (McCabe *et al.* 1989; Pan *et al.* 1990). However, in many cases a CRM mechanism cannot be identified with any certainty. Other processes must obviously be taken into account. For example, Katz *et al.* (2000) have recently demonstrated that the widespread CRM in the Vocontian trough (SE France) is connected to the burial and diagenetic alteration of smectite.

In epimetamorphic sedimentary covers from many mountains belt, the thermal history is poorly constrained and remagnetizations can possibly be regarded as TRMs. Slow cooling during post-metamorphic erosion and uplift has the result of lowering and broadening the blocking temperature (T_b) range of magnetic minerals (Pullaiah *et al.* 1975; Dunlop *et al.* 2000). The magnetization is blocked in a certain temperature interval around T_b. Secular variations are averaged because of cooling, and all the rocks formed before the thermal event record the same geomagnetic field (GMF), provided that the blocking temperature spectra are similar. Samples at a higher crustal level (now at higher altitude in a mountain belt) are magnetized before those at a lower crustal level (altitude). The cooling rate of metamorphic rocks can allow them to record variations of the GMF versus their blocking temperature spectra and versus altitude. Very slowly cooled metamorphic rocks have recorded the apparent polar wander path (Piper 1981; Dodson & McClelland-Brown 1985). Faster cooled rocks (i.e. intrusions) have been used to study the record of field reversal (Dodson *et al.* 1978; Williams & Fuller 1982). In epimetamorphic rocks with an intermediate cooling rate, it is also known that several successive polarities can be retrieved using stepwise thermal demagnetization (Rochette *et al.* 1992; Ménard & Rochette 1992; Crouzet *et al.* 1997, 1999). Unlike magnetostratigraphy, where the oldest (youngest) polarity is found in the lowest (highest) part of a stratigraphically continuous section, the youngest (oldest) polarity may be found at the lowest (highest) part of a metamorphic pile, provided that successive polarities are recorded during cooling (Fig. 1).

The present contribution deals with pyrrhotite-bearing limestones from a section located in the Tethyan Himalaya (Hidden Valley, Central Nepal). It focuses on the remagnetization in these metasediments and demonstrates its thermal origin.

GEOLOGICAL SETTING

The Himalayan belt is the result of the collision of India with Eurasia and extends for over 2500 km in the E–W and 250–320 km in the N–S directions between the Tibetan plateau and the Gangetic plain. It is traditionally separated into five major tectonometamorphic units from north to south (Gansser 1964 and Fig. 2): (1) the Indus–Tsangpo suture zone, (2) the Tethyan Himalayan (TH) sediments, which are considered as the stratigraphic cover of (3) the High Himalayan crystallines (HHC). The latter is thrust over (4) the Lesser Himalaya and (5) the Sub-Himalaya (Siwaliks), which represents the foreland basin.

The TH comprises a continuous sedimentary sequence ranging from Cambro-Ordovician to Eocene (Bodenhausen *et al.* 1964; Bordet *et al.* 1971; Fuchs 1977; Bassoulet & Mouterde 1977; Garzanti & Pagni Frette 1991). It is generally interpreted as shelf sediments deposited on the passive northern margin of the Indian plate (Bassoullet *et al.* 1980; Brookfield 1993). To the south, the TH is commonly separated from the polymetamorphic basement of the HHC by north-dipping normal faults that constitute the South Tibetan Detachment System (STDS), first suggested by Caby *et al.* (1983) and now largely accepted since

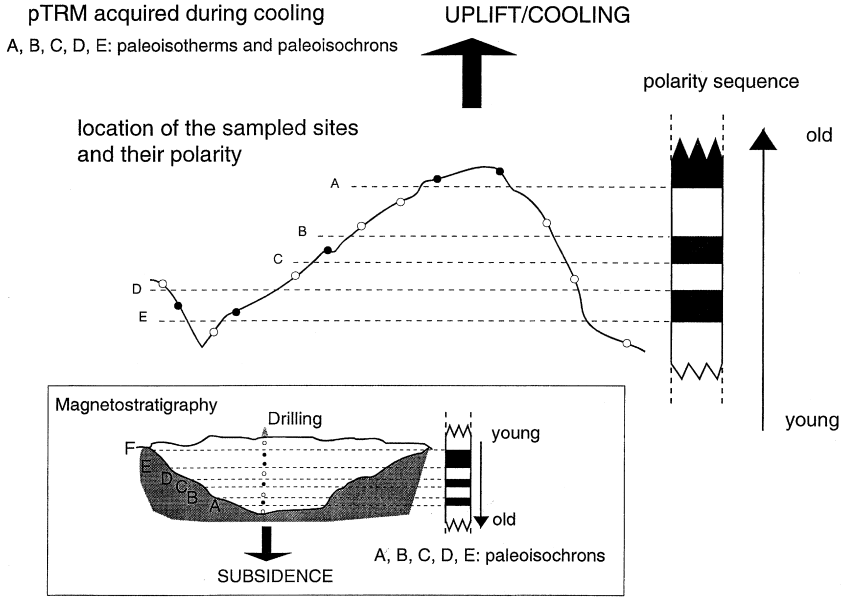

Figure 1. Successive pTRM acquisition model during uplift and cooling of a metamorphic unit compared to the successive polarities acquired during deposit of sediments (magnetostratigraphy).

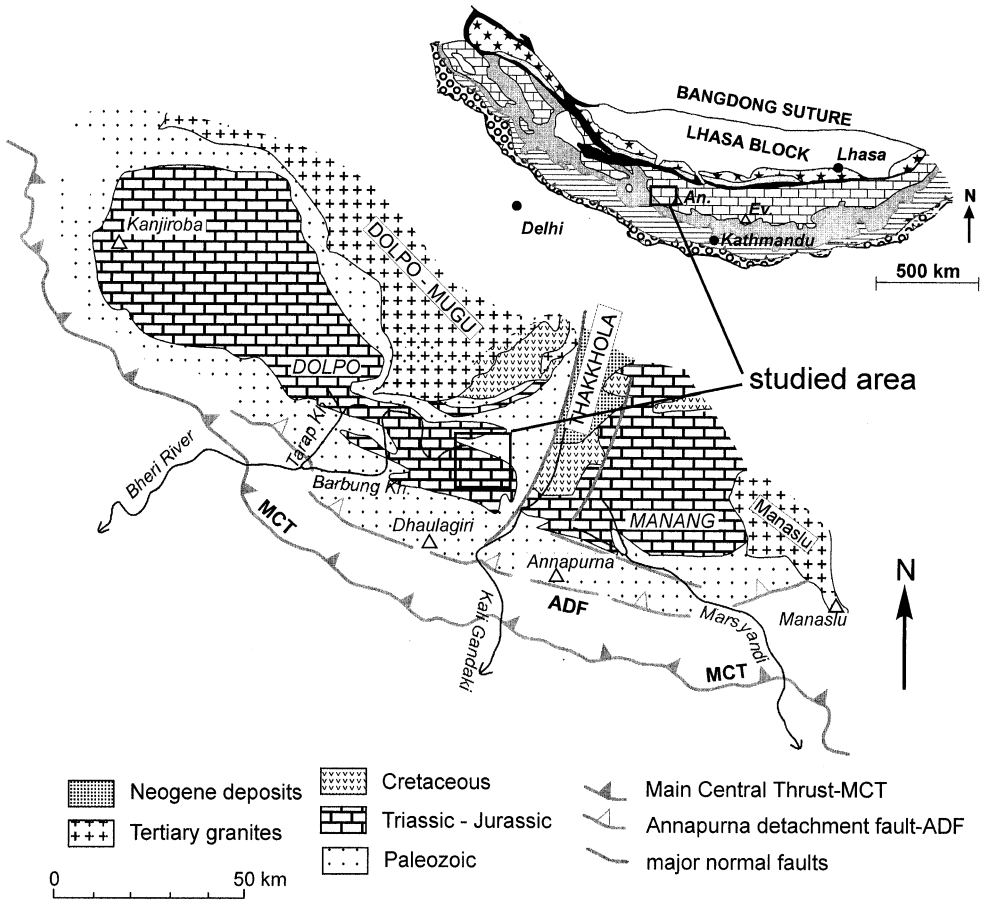

Figure 2. Geological map of the Thakkhola area (redrawn after Garzanti *et al.* 1994) in the Himalayan belt.

the work of Burchfield *et al.* (1992). The high-grade metamorphism of the HHC decreases progressively and quite rapidly from S to N in the TH. The grade of metamorphism varies laterally and may affect different stratigraphic levels (Gansser 1981; Fuchs 1982; Garzanti *et al.* 1994; Ratschbacher *et al.* 1994). The TH sediments are locally intruded by Miocene leucogranites (Le Fort 1986; England *et al.* 1992; Le Fort & France Lanord 1995; Guillot *et al.* 1999).

In the eastern Dolpo and Thakkhola areas (Fig. 2) the so-called Thakkhola graben is a major morphological unit. It is a late orogenic extensional structure running N–S between the Annapurna and Dhaulagiri ranges. In this structural depression, Cretaceous and Tertiary sediments are preserved. Elsewhere in these areas, the stratigraphic column ranges from Cambro-Ordovician to middle Jurassic (Fuchs 1967; Colchen *et al.* 1986).

The eastern Dolpo–Thakkhola region has undergone several phases of fold-and-thrust-type deformation with contrasting vergence (Colchen 1975; Brown & Nazarchuk 1993; Godin *et al.* 1999a,b). In the environs of Hidden Valley, the Cambrian to Jurassic TH sediments were subjected to very low- to medium-grade thermal metamorphism (temperatures around 275–330 °C from illite crystallinity data) during the Himalayan orogeny (Schneider & Masch 1993; Garzanti *et al.* 1994). Unfortunately, in Hidden Valley no numerical dates for the age of metamorphism or palaeotemperatures are available in the literature. Preliminary K/Ar dating on phyllites and illite crystallinity studies (Crouzet *et al.*, in preparation) indicate an age of $\sim 29.1 \pm 1.8$ Myr and a Kübler index of ~ 0.336. This age is probably a mixed age (that is, between the age of detrital illites and the age of the thermal event). Illite crystallinity may indicate temperatures during the thermal event of ~ 290–340 °C. The age of the low-grade metamorphism affecting the TH in Western Nepal is still debated (see the 'Age of the remagnetization' section below).

SAMPLING AND MEASUREMENTS

A portable rock drill was used to obtain 2.5 cm diameter cores, which were oriented using a magnetic compass. Bedding measurements were performed for tectonic correction. Generally about 10 cores were drilled at each site. In total around 300 oriented cores from 28 sites were taken from Hidden Valley within an area of 3×10 km (Fig. 3). Three different formations were sampled: 10 sites in the Tilicho Lake Formation (lower Carboniferous limestones), nine sites in the Tamba Kurkur Formation (lower Triassic limestones) and nine sites in the Mukut Limestone (Middle Triassic).

Before treatment, the anisotropy of susceptibility (AMS) was measured using a Kappabridge KLY-2 (Agico) in order to detect possible correlation between the rock magnetic fabric and the remanence directions. One specimen per site was used for isothermal remanence (IRM) acquisition in a stepwise increasing DC field up to 2.5 T at room temperature using an MMPM9 pulse magnetizer (Magnetic Measurements). Subsequent thermal demagnetization (THD) was carried out in 17 steps up to 680 °C. Detailed stepwise alternating field demagnetization (AFD) as

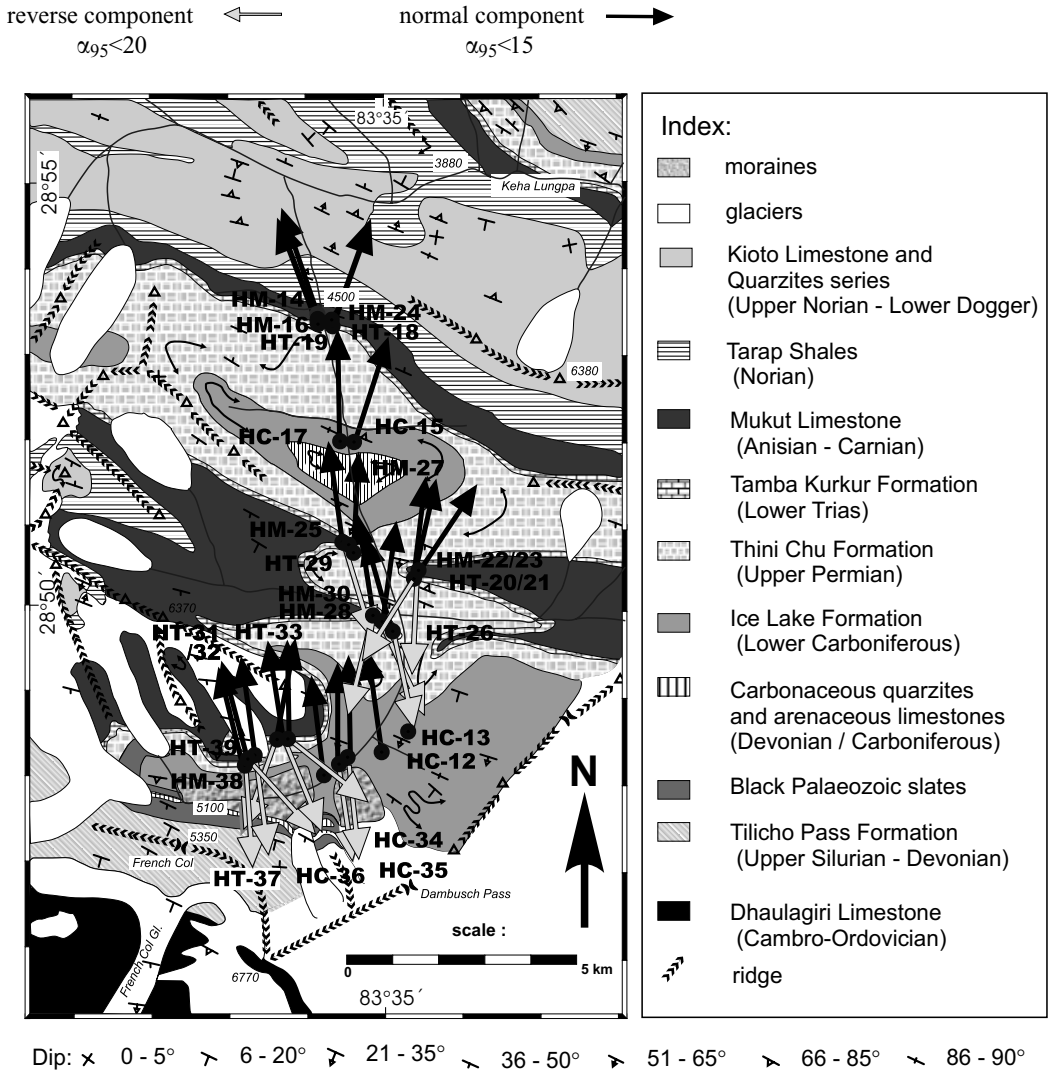

Figure 3. Geological map of Hidden Valley (based on Fuchs 1967) with directional analysis of ChRM. Black (white) arrows: normal (reverse) components.

well as THD was performed for one pilot sample (twin samples from one core) from each site. The AFD of natural remanent magnetization (NRM) was performed using an automatic degausser (2G600) coupled with a three-axis SQUID magnetometer (RF SQUID 755 R, 2G Enterprises). This magnetometer was also used for measuring the magnetization remaining after each heating step. The noise level is estimated to be lower than 5×10^{-6} A m^{-1} for 10 cm^3 samples on each axis with a directional repeatability of around 2°. Based on the results of pilot demagnetization, the remaining samples were treated thermally first with a 50 °C step between 100 and 250 °C and then with steps of 10 °C until all the magnetization was removed. A second thermal procedure was used for two or three samples per site using the following steps: 100, 180, 210, 235 and 250 °C, followed by 4–5 °C steps up to 350 °C. All the thermal treatments were performed using an MMTD 60 furnace (Magnetic Measurements). Temperatures shown in this paper are based on thermal calibration performed during demagnetization experiments using a Ni/Cr thermocouple placed into dummy samples. The furnace and the SQUID magnetometer were hosted in a three-axis Helmholtz coil system for additional field compensation. This avoids the possibility of a strong viscous remanent magnetization between heating and subsequent magnetization measurement. After each heating step, the bulk susceptibility was measured using a Kappabridge KLY-2 in order to detect alteration during demagnetization. Thermal susceptibility runs were carried out in order to confirm our previous magneto-mineralogical identification using a CS2 heating unit coupled with a Kappabridge KLY-2. For those measurements, samples with high bulk susceptibility were selected, crushed manually in a brass mortar under ethyl alcohol to avoid oxidation and other possible mineralogical changes, and finally air-dried. A heating rate of 10 °C min^{-1} was used in order to minimize possible alterations during experiments.

RESULTS

Magnetic mineralogy

IRM acquisition curves show that saturation is never reached below 1 T. Subsequent THD exhibits a strong decay between 300 and 350 °C. AFD of NRM up to 140 mT reveals the loss of

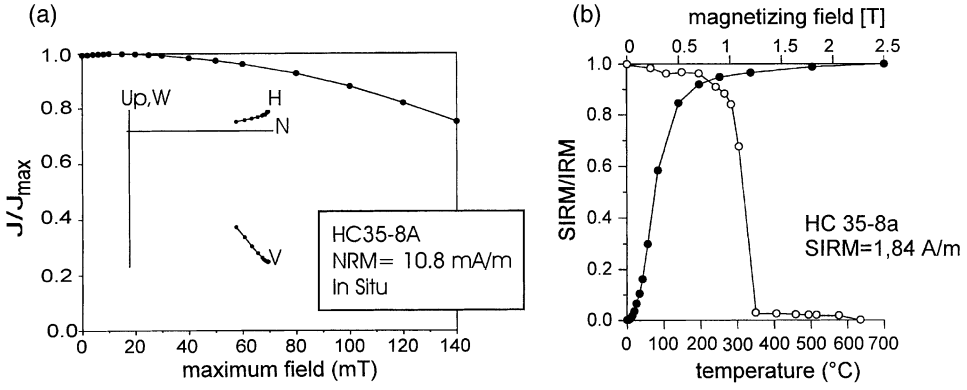

Figure 4. (a) AF demagnetization of NRM; (b) IRM acquisition and subsequent thermal demagnetization.

only 30 per cent of the initial magnetization (Fig. 4). In some samples, 5 per cent of the initial IRM remained after 400 °C during thermal treatment. This was removed at around 580–600 °C, indicating a very small magnetite content, or at around 650–700 °C, indicating the presence of some haematite.

Susceptibility versus temperature curves measured in air commonly showed a maximum of susceptibility (Hopkinson peak) followed by a drop of susceptibility around the Curie temperature of pyrrhotite (320–330 °C; Fig. 5). A sudden rise around 500 °C indicates the formation of magnetite due to heating. Many heating curves exhibit a plateau of susceptibility between 350 and 500 °C that can be interpreted as the presence of some initial magnetite. The newly formed magnetite dominates the initial magnetic mineralogy during cooling. This is the first pyrrhotite identification using thermal dependence of susceptibility in the Tethyan Himalayan Sedimentary Series. It confirms the occurrence of pyrrhotite as the major carrier of magnetization, independent of stratigraphic level, in this series, as already demonstrated by Appel *et al.* (1991).

During THD, the bulk susceptibility remains unchanged until around 290–320 °C, attesting to the stability of pyrrhotite up to this temperature. Between 300 and 360 °C, the bulk susceptibility increases slowly. This increase does not exceed 15 per cent in most of the samples. A dramatic rise in susceptibility occurs after 350–400 °C, probably indicating the transformation/oxidation of the initial pyrrhotite (and pyrite) into magnetite.

Analysis of NRM

Thermal demagnetization was performed in order to determine the pyrrhotite component. Surprisingly, several components can be isolated in the pyrrhotite unblocking temperature range (200–330 °C, Tables 1 and 2). The separated remanence directions (normal/reverse) vary with altitude. It is also possible to retrieve several antiparallel components as a function of temperature during thermal demagnetization of a single sample. At higher altitudes (4920–5500 m), the first component recorded (highest temperature) is reverse (R_1). At a lower temperature a normal component can be clearly extracted (N_1). For sites sampled at lower altitudes (4700–4900 m), the reverse component with high unblocking temperature disappears but a small reverse component (R_2), demagnetized in a narrow intermediate temperature range only (Table 2), can be identified in some samples

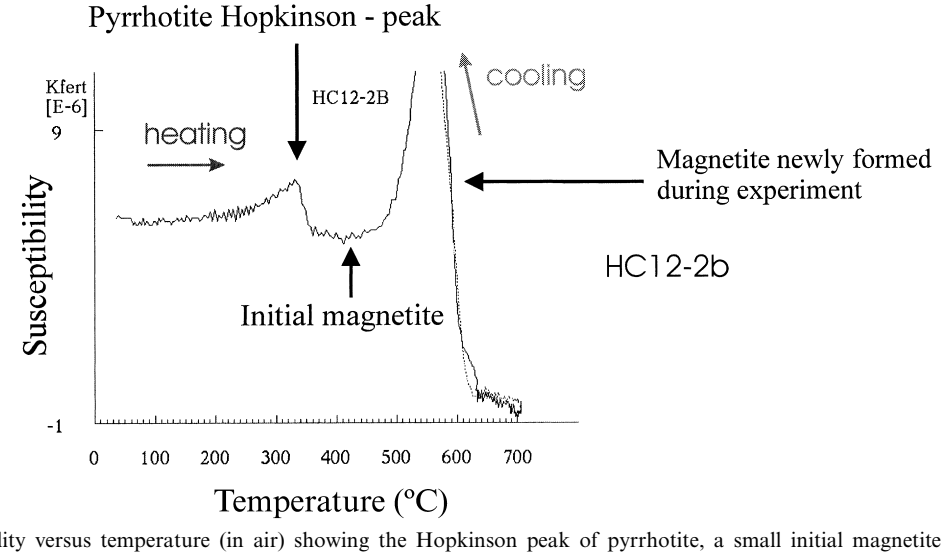

Figure 5. Susceptibility versus temperature (in air) showing the Hopkinson peak of pyrrhotite, a small initial magnetite content and the new formation of magnetite during heating. The paramagnetic contribution was eliminated using the method of Hrouda (1994).

Table 1. Site mean directions and regional mean directions for components R_1 (reverse polarity) and N_1+N_2 (normal polarity). Lat, Long and Alt: geographical latitude, longitude and altitude of sampled sites; No: total number of samples; N: number of samples used for Fisher statistics; D: declination; I: inclination; α_{95}: confidence angle for 95 per cent level; k: precision parameter.

Site name	Lat (N)	Long (E)	Alt (m)	No	Normal component (N_1+N_2)					Reverse component (R_1)				
					D	I	α_{95}	k	N	D	I	α_{95}	k	N
HM14	28°52.44′	83°35.31′	4470	10	341	67	10	26	9					
HM16	28°52.38′	83°35.31′	4475	8	no significant result (scattering direction)									
HT19	28°52.36′	83°35.32′	4480	9	339	68	6	113	7					
HM24	28°52.38′	83°35.45′	4570	10	no significant result (scattering direction)									
HC15	28°51.62′	83°35.18′	4595	9	18	60	3	279	9					
HC17	28°51.62′	83°35.12′	4600	9	359	62	3	278	8					
HT18	28°52.35′	83°35.48′	4600	9	20	67	8	66	6					
HT29	28°50.69′	83°35.00′	4820	7	8	56	6	113	6					
HM25	28°50.82′	83°34.94′	4840	9	356	63	4	183	9					
HT20	28°50.40′	83°35.53′	4840	10	9	16	8	41	9					
HT21	28°50.41′	83°35.57′	4860	10	no significant result (scattering direction)									
HM27	28°50.76′	83°34.95′	4870	7	no significant result (very low intensity)									
HC13	28°48.89′	83°35.28′	4880	9	no significant result (very low intensity)									
HT26	28°49.95′	83°34.95′	4880	10	353	70	10	147	3					
HC34	28°48.60′	83°34.47′	4910	7	353	59	4	226	7					
HC35	28°48.63′	83°34.51′	4910	10	0	55	5	113	10	172	−63	8	1078	2
HM22	28°50.49′	83°35.58′	4910	9	34	−3	7	50	9					
HC36	28°48.74′	83°34.61′	4920	9	359	48	7	73	7	175	−59	6	127	6
HM23	28°50.51′	83°35.60′	4920	8	5	28	9	36	7	183	−19	33	7	5
HC12	28°48.41′	83°35.00′	4940	8	352	64	4	174	8	137	−64	40	41	2
HM28	28°49.91′	83°34.88′	4940	9	8	60	4	148	9	193	−68	13	51	4
HM30	28°49.95′	83°34.84′	4970	10	351	67	5	113	9	154	−72	18	27	4
HT39	28°48.57′	83°32.19′	5410	9	351	57	4	202	7	165	−71	9	50	7
HT37	28°48.51′	83°32.10′	5440	10	346	51	7	55	10	174	−60	9	28	10
HM38	28°48.57′	83°32.12′	5470	10	345	54	5	94	9	138	−59	8	45	9
HT31	28°48.85′	83°32.53′	5520	8	11	45	10	45	6	200	−50	13	28	6
HT33	28°48.85′	83°32.68′	5535	7	349	63	10	47	6	139	−64	19	14	6
HT32	28°48.86′	83°32.52′	5550	9	358	54	7	57	9	157	−64	7	84	7
All sites (except HT20, HM22, HM23)				23	357.2	59.2	3.6	85.7	19	167.4	−64.5	7.8	44.0	9

in between two normal components (N_1 at high temperature and N_2 at low temperature). In many other samples, no intensity change is observed during thermal demagnetization in the R_2 temperature range. This plateau-like behaviour is interpreted as a record that took place within a few degrees cooling during the R_2 polarity interval. Of course, in this case it is impossible to extract it. As the number of significantly separated R_2 directions is very low, the mean direction determined is not taken into account in this paper. At lowest altitudes between 4450 and 4700 m, only a normal component is seen (Fig. 6). In total, four components (R_1, N_1, R_2, N_2) were extracted using principal component analysis (Kirschvink 1980). The maximum angular deviation of the least-squares fits rarely exceeds 10. A negative fold test (99 per cent significant after McElhinny 1964) shows that these are secondary magnetizations post-dating the major folding of the studied area. The mean directions at each site and for the entire area were calculated using Fisher statistics. The site mean directions generally have $\alpha_{95}<11^\circ$ and $k>30$ (Table 1). Of a total of 28 sites, five were rejected from the directional analysis due to very low magnetization intensity or wide scattering of remanent directions, probably due to the effect of anisotropy. For the other 23 sites, no effect of anisotropy on the remanence direction was detected by AMS measurements. As R_2 does not occur in all the samples and as the directions of N_1 and N_2 are very similar, the directional analyses of N_1 and N_2 were performed together. For calculation of the regional mean directions (R_1 and N_1+N_2), sites with fewer than four specimen data were rejected. Sites HT20, HM22 and HM23 are not included in the mean calculation because they show anomalous directions with a very low inclination (possibly due to a recent collapse of the site area). From stable remanence directions carried by pyrrhotite, the amount of block rotation around horizontal and vertical axes can be estimated. The remanence declination is compatible with a Tertiary acquisition age (see Discussion). Declinations (R_1: 167.4°; N_1+N_2: 357.2°) show no obvious rotation around a vertical axis with respect to the stable Indian plate based on the Tertiary apparent polar wander path (Besse & Courtillot 1991). However, the inclination is not consistent with the expected range ($I_{exp}<45$–50°). The Main Central Thrust ramping model (Appel *et al.* 1991; Rochette *et al.* 1994) can be invoked to explain our observations. Whilst the α_{95} confidence cones overlap, R_1, N_1 and N_2 differ slightly in inclination. This tendency of inclination increase with age of remanence acquisition is consistent with tilting towards the north during magnetization acquisition (Fig. 7). The total amount of this tilting is around 25° if the magnetization age is 20 Ma but 41° if the magnetization was acquired at 40 Ma. We must bear in mind that we are recording only the total motion and that our observations are probably the sum of several deformations.

Table 2. Unblocking temperature ranges for the different components extracted. T_C: Curie temperature of pyrrhotite (~330 °C); RT: room temperature. A question mark indicates that the lower polarity should have been recorded but was not clearly evidenced during thermal demagnetization.

Site name	Alt (m)	N_2 $T°$ range	R_2 $T°$ range	N_1 $T°$ range	R_1 $T°$ range
HM14	4470	RT–T_C			
HT19	4480	RT–T_C			
HC15	4595	RT – 300	300–310	310–T_C	
HC17	4600	RT – 290	290–300	300–T_C	
HT18	4600	RT – 290	290–310	310–T_C	
HT29	4820	RT – 295	295–310	310–T_C	
HM25	4840	RT – 305	305–315	315–T_C	
HT20	4840	RT – 300	300–315	315–T_C	
HT26	4880	RT – 295	295–320	320–T_C	
HC34	4910	RT – 295	295–305	305–T_C	
HC35	4910		?	? – 320	320–T_C
HM22	4910	RT – 300	300–310	310–T_C	
HC36	4920		?	? – 315	315–T_C
HM23	4920	RT – 295	295–310	310–T_C	
HC12	4940		?	? – 320	320–T_C
HM28	4940		?	? – 310	310–T_C
HM30	4970		?	? – 315	315–T_C
HT39	5410			RT – 300	300–T_C
HT37	5440			RT – 310	310–T_C
HM38	5470			RT – 310	310–T_C
HT31	5520			RT – 300	300–T_C
HT33	5535			RT – 300	300–T_C
HT32	5550			RT – 295	295–T_C

DISCUSSION

The thermal origin of the remagnetization

The directional analysis of pyrrhotite components presented in this paper shows that antiparallel directions occur in samples as a function of temperature and at the scale of sites as a function of elevation. To explain this observation, self-reversal processes are very unlikely because only monoclinic pyrrhotite (no γ-transition in thermomagnetic runs) and no changes in the bulk susceptibility during THD are observed. It is well known since the work of Néel (1949) that the magnetization is acquired when the relaxation time becomes larger than the time of the experiment. The evolution of the relaxation time is mainly controlled by two parameters: the volume of the grain and the temperature. Using only the volume of the grains, it will produce a CRM, while using only temperature, it will produce a TRM. Two models are proposed to explain the occurrence of antiparallel components in the studied samples (Fig. 8). Antiparallel components in CRM are not common but have been reported by Katz *et al.* (2000) and Bailly *et al.* (2000). The following model is idealistic and natural processes are probably much more complicated. The growth of magnetic grains in a rock is not instantaneous and can extend over several reversals of the GMF. When the volume of the grains is increasing during metamorphic growth, the grains will acquire magnetization when crossing through their blocking volumes (V_1). If a reversal of the GMF occurs while grains are still growing, new grains reaching their blocking volume (V_2) will record a magnetization in the opposite direction to the previous one. Of course, grains that have exceeded the blocking volume may still continue to grow but the magnetization is already blocked. This process can continue throughout the time taken by the crystallization process. As $V_1 > V_2 \ldots > V_n$, the unblocking temperature of V_1 (T_{ub1}) is higher than the unblocking temperature of V_2 (T_{ub2}). Therefore, $T_{ub1} > T_{ub2} > \ldots > T_{ubn}$ when $V_1 > V_2 > \ldots > V_n$ as long as the grains do not exceed the single domain–multidomain transition. Thus, using thermal demagnetization, it is theoretically possible to retrieve several antiparallel components recorded in one sample. However, in order to explain the polarity versus altitude dependence, it is necessary to assume that the grains grow at different times, which vary with their actual altitude. This seems quite unlikely. The pTRM model (Figs 1 and 8) thus seems very appropriate to explain the behaviour of the magnetization in Hidden Valley, especially the differences in polarities between the upper, middle and lower parts of the section (Fig. 9). As cooling occurs, samples from the upper part start to record a reverse polarity (R_1). At the same time the samples in the middle and lower parts are unable to record this R_1 event as the temperature is still too high (> 330 °C = Curie temperature of pyrrhotite). During further cooling, a reversal of the GMF occurs and samples from the upper and middle parts now record a normal polarity (N_1). Again, the GMF changes and samples from the middle part record it (R_2). This polarity event seems not to have been recorded by the samples from the upper parts because the temperature is already below 250 °C, in a range where almost no more magnetization is acquired. The R_2 polarity event is not recorded by samples from the lower part either because the temperature is still above 330 °C. Later the GMF reverses again and samples from the middle and lower parts record a normal polarity (N_2) at this time.

Towards the absolute temperature/time correlation

Compiling the data from the upper, middle and lower parts of the studied area, it is possible to establish a polarity sequence. Assuming that all the polarity intervals are recorded during

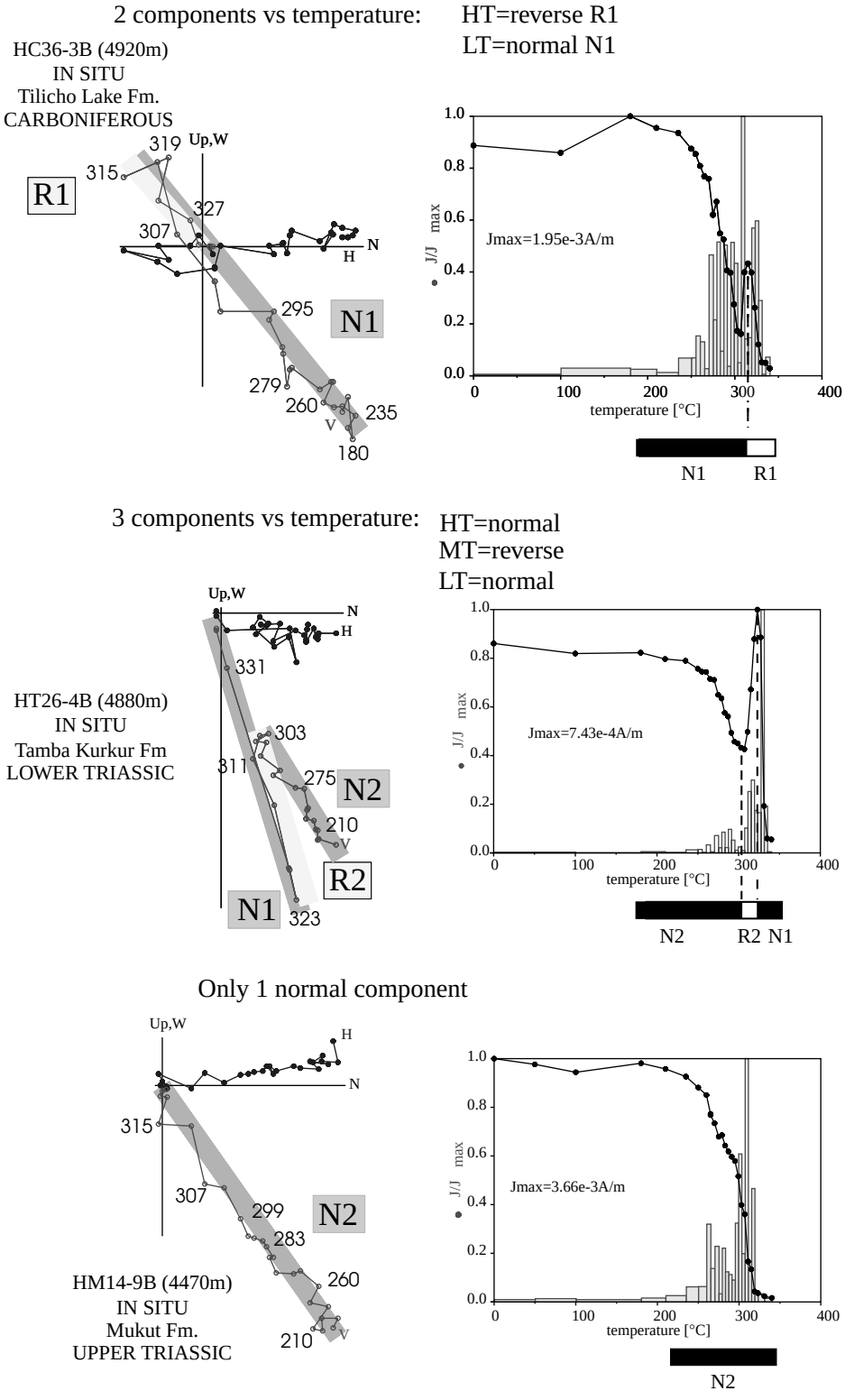

Figure 6. Thermal demagnetization (temperature values in °C) of NRM showing several antiparallel components and the evolution versus altitude.

cooling (duration of chron × cooling rate $> \sim 5$ °C, the temperature steps during THD) and assuming continuous cooling (no reheating), a polarity sequence is built up. This polarity sequence is built up for samples taken from 4920 m above mean see level (site HC36) and presented in Table 3. The R_2 component is well evidenced in the 290–320 °C range in the samples from the middle part. This component should also be recorded by samples from the upper part. The THD of samples from the upper part show no R_2 component in the unblocking temperature range except in a few samples from the base of the upper part, where a slight plateau-like behaviour, defined by only two measurement points, occurs. This may represent a

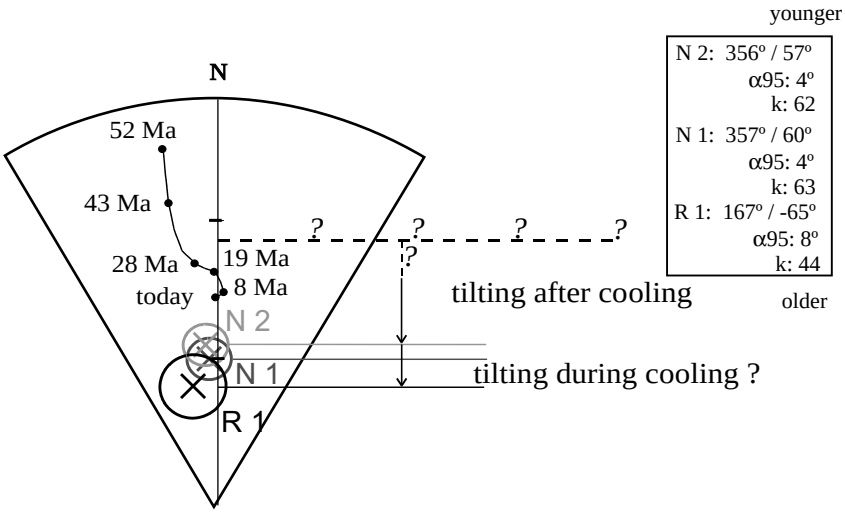

Figure 7. Stereoplot of R_1, N_1 and N_2 with confidence cone at 95 per cent compared to the APWP from stable India after Besse & Courtillot (1991). R_1, N_1 and N_2 mean directions are indicated. The tendency (Inc R_1 > Inc N_1 > Inc N_2) is possibly consistent with tilting towards the north during magnetization acquisition.

Table 3. Polarity sequence versus temperature at 4920 m altitude. The temperatures of N_1/R_2 and R_2/N_2 are estimated values (see explanation in the text). Corresponding natural blocking temperatures are calculated after Crouzet *et al.* (1999).

	R_1/N_1	N_1/R_2	R_2/N_2
Unblocking T (°C) in the oven	315	260	240
Natural blocking T (°C)	307	228	201

record of R_2 in the 200–260 °C temperature range. According to the THD, R_2 cannot be recorded by samples from site HC36 at temperatures higher than around 250–260 °C. This temperature is taken as the highest possible one for the occurrence of the R_2 component in samples from the upper part. In the middle part, R_2 is identified over 15–20 °C, so the transition from R_2 to N_2 should be recorded by samples from the upper part between 240 and 260 °C.

Due to the difference between the time of magnetization acquisition in natural conditions ($\sim 10^{12}-10^{13}$ s) and the demagnetization time in the laboratory ($\sim 10^{3}$ s), a correction is needed to retrieve the natural temperatures at which each reversal occurs (Crouzet 1997; Dunlop *et al.* 2000). As the sensitivity of this correction to variations of natural cooling rate is very small, it is not useful to test different hypotheses in the geologically realistic 10–100 °C Myr^{-1} range (Crouzet *et al.* 1999).

Age of the remagnetization

The next step will be to compare this sequence with the magnetostratigraphic timescale in order to obtain a precise cooling path. For this we must have an idea of the age of the metamorphic event affecting Hidden Valley. This metamorphism may be Eohimalayan (45–35 Ma) as in Zanskar or Spiti (Bonhomme & Garzanti 1991; Wiesmayr & Grasemann 1999) or Neohimalayan ($\sim$20 Ma) or related to the emplacement of the Mugu granite ($\sim$16 Ma as suggested by Ar/Ar data from micas; Guillot *et al.* 1999). The temperature time history of the studied

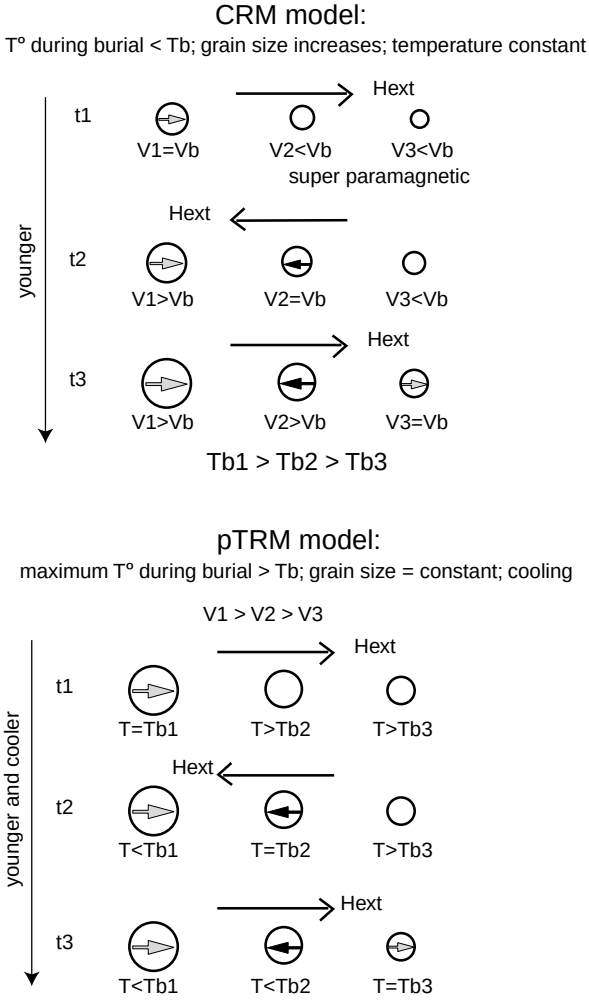

Figure 8. CRM and TRM models to explain the occurrence of successive polarities versus temperature during thermal demagnetizations. The CRM model is based on the blocking-volume concept while the TRM model is based on the blocking-temperature concept.

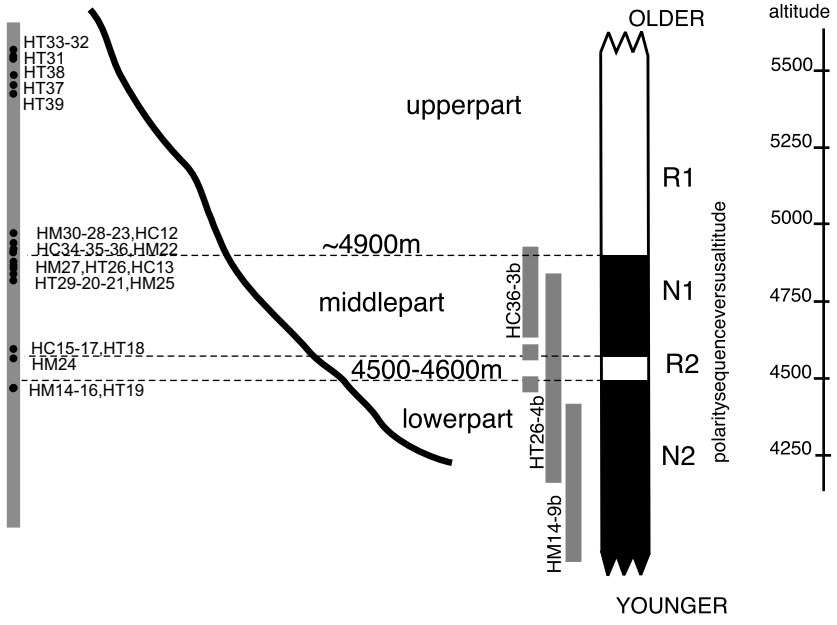

Figure 9. Synthetic polarity sequence versus altitude deduced from thermal demagnetization and altitude of samples. The site locations refer to the altitude scale on the right-hand side. Grey lines represent the polarity sequence recorded by samples presented in Fig. 6.

area is not constrained. We made a compilation of the geochronological data on the Dolpo–Manang area published in the literature. Unfortunately, for this area no data are available from the TH metasediments, except those from the vicinity of granites (see Guillot *et al.* 1999 for a review) or the South Tibetan detachment (Coleman & Hodges 1998; Godin *et al.* 1999a). Only Ar/Ar dating on illite from Zanskar (Bonhomme & Garzanti 1991) and Spiti (Wiesmayr & Grasemann 1999), giving ages between 47 and 42 Ma, is available in the TH far from granites and the HHC. Hence, the age of the thermal event in the Tethyan sedimentary cover remains a topic for debate. An Eohimalayan (45–35 Ma) metamorphism or a Neohimalayan (25–15 Ma) event associated with granite emplacement is possible. New geochronological and thermal constraints from the Tethyan sedimentary cover, away from the South Tibetan Detachment and from granites, are desirable.

CONCLUSIONS

The thermoremanent nature magnetization carried by pyrrhotite implies that the temperature reached during the metamorphic event was >320–330 °C (to a maximum of 400 °C). This thermal event cannot be explained by the thickness (less than 3 km) of the original sedimentary cover alone unless there existed a very high vertical thermal gradient, probably associated with granite emplacement or significant fluid circulation. If the latter processes occurred, the magnetization age could be between 25 and 15 Ma. However, if the high thermal gradient hypothesis is rejected, and a 'normal' value for the geothermal gradient is assumed, the burial reached by sedimentary cover in Hidden Valley is estimated to be ~ 11 km. This implies the existence of a thrust carrying unmetamorphosed material over the studied area, probably in Upper Eocene to Oligocene time. Such timing is suggested by (1) geochronological data from the Kali Gandaki Valley in the HHC [Ar/Ar on hornblende at around 37 Ma (Vannay & Hodges 1996) and U/Pb on monazite and zircon at around 35 Ma (Godin *et al.* 1999b)], (2) the K/Ar and Ar/Ar ages on phyllites in the Zanskar and Spiti areas (Bonhomme & Garzanti 1991; Wiesmayr & Grasemann 1999), and (3) the tectonometamorphic evolution of the Himalayan metamorphic core proposed by Vannay & Hodges (1996).

This study demonstrates the thermoremanent origin of remagnetization carried by pyrrhotite in Hidden Valley (Central Nepal) and attempts to estimate more precisely the peak temperature reached during metamorphism. A chemical origin of remagnetization is very unlikely because the high-temperature component recorded in the studied samples is successively normal and reverse as a function of altitude. The occurrence of antiparallel components recorded by metasediments throughout the blocking temperature spectra and for all elevations is the basic and very powerful argument in favour of a thermal origin of the remagnetization. Vertical sections are then very useful for differentiating CRM and TRM remagnetizations. The NRM components with opposite polarity are interpreted as the record of a succession of geomagnetic field reversals during post-metamorphic cooling. Directional analysis suggests a lack of any obvious vertical-axis rotation with respect to stable India. The measured inclinations, however, deviate significantly from the expected direction by at least 20–25° depending on the remagnetization age. In order to date precisely the magnetization, more detailed geochronological investigations are needed. Tethyan Himalaya metasediments are ideal for this kind of study because of the large exposed thickness of suitable formations, which occur over a distance of more than 2000 km.

ACKNOWLEDGMENTS

This work was funded by the German Research Council (DFG), project AP 34/13-1. We thank the editor and anonymous reviewers for helpful comments.

REFERENCES

Appel, E., Müller, R. & Widder, R.W., 1991. Paleomagnetic results from the Tibetan Sedimentary Series of the Manang area (north central Nepal), *Geophys. J. Int.,* **104,** 255–266.

Bailly, S., Aubourg, C. & Pozzi, J.-P., 2000. Tertiary normal remagnetization of the Jurassic facies from south Subalpine Chains, *EGS, 25th General Assembly, Geophysical Research Abstracts,* **2,** 66.

Bassoulet, J.P. & Mouterde, R., 1977. Les formations sédimentaires Mésozoïques du domaine tibétain de l'Himalaya du Népal, *Coll. Int. CNRS,* **268,** 53–60.

Bassoullet, J.P., Boulin, J., Colchen, M., Marcoux, J., Mascle, G. & Montenat, C., 1980. Evolution des domaines téthysiens au pourtour du bouclier indien du carbonifère au Crétacé, *Géologie des Chaînes Alpines Issues de la Téthys, Colloque C5 du 26ème Congrès Géologique Int., Paris, Mém. BRGM.,* **115,** 180–198.

Besse, J. & Courtillot, V., 1991. Revised and synthetic apparent polar wander paths of the African, Eurasian, North American and Indian plates, and true polar wander since 200Ma, *J. geophys. Res.,* **96,** 4029–4050.

Bodenhausen, J.W.A., De Booy, T., Egeler, C.G. & Nijhuis, H.J., 1964. On the geology of central and west Nepal: a preliminary note, *Rept 22nd Int. Geol. Congr.,* Part 11, pp. 101–122, Publisher?, Delhi.

Bonhomme, M. & Garzanti, E., 1991. Age of metamorphism in the Zanskar Tethys Himalaya (India), *Géol. Alpine. Mem. HS,* **16,** 15–16.

Bordet, P., Colchen, M., Krummenacher, D., Le Fort, P., Mouterde, R. & Rémy, J.M., 1971. *Recherches Géologiques Dans l'Himalaya Du Népal, Région de la Thakkhola,* CNRS, Paris.

Brookfield, M.E., 1993. The Himalayan passive margin from Precambrian to Cretaceous time, *Sed. Geol.,* **84,** 1–35.

Brown, R.L. & Nazarchuk, J.H., 1993. Annapurna detachment fault in the Greater Himalaya of Central Nepal, in *Himalayan Tectonics,* eds Treloar, P.J. & Searle, M.P, *Geol. Soc. Lond. Spec. Publ.,* **74,** 461–473.

Burchfield, B.C., Chen, Z., Hodges, K.V., Liu, Y., Royden, L.H., Deng, C. & Xu, J., 1992. The southern Tibetan Detachment System, Himalayan orogen: extension contemporaneous with and parallel to shortening in a collisional mountain belt, *Geol. Soc. Am. Spec. Pap.,* **269,** 1–41.

Caby, R., Pécher, A. & Le Fort, P., 1983. Le chevauchement central himalayen: nouvelles données sur le métamorphisme inverse à la base de la dalle du Tibet, *Rev. Géol. Dyn. Geogr. Phys.,* **24,** 89–100.

Colchen, M., 1975. Tectonique des series tibétaines, in *Recherches Géologiques Dans l'Himalaya Du Népal, Region Du Nyi-Shang,* pp. 67–97, eds Bordet, P., Colchen, M. & le Fort, P., CNRS, Paris.

Colchen, M., Le Fort, P. & Pêcher, A., 1986. Annapurna, Manaslu, Ganesh Himal, *Notice de la Carte Géologique Au 1/200 000éme. Recherches Géologiques Dans l'Himylaya Du Népal,* CNRS, Paris.

Coleman, M. & Hodges, K., 1998. Contrasting Oligocene and Miocene thermal histories from the hanging wall and footwall of south Tibetan detachment in the central Himalaya from 40Ar/39Ar thermochronology, Marsyandi Valley, Central Nepal, *Tectonics,* **17,** 726–740.

Crouzet, C., 1997. Le thermopaléomagnétisme: méthodologie et applications (tectonique, thermique et géochronologique) à la zone dauphinoise interne (Alpes occidentals, France), *Géol. Alpine Mém. HS,* **27,** 1–197.

Crouzet, C., Rochette, P., Ménard, G. & Prévot, M., 1997. Acquisition d'aimantations thermorémanentes partielles successives portées par la pyrrhotite monodomaine lors du refroidissement de la zone dauphinoise interne (Alpes occidentales, France), *C. R. Acad. Sci., Paris,* **II,** 325**,** 643–649.

Crouzet, C., Ménard, G. & Rochette, P., 1999. High-precision three-dimensional paleothermometry derived from paleomagnetic data in an alpine metamorphic unit, *Geology,* **27,** 503–506.

Dodson, M.H. & McClelland-Brown, E., 1985. Isotopic and paleomagnetic evidence for rate of cooling, uplift and erosion, in *The Chronology of Geological Record,* pp. 315–325, ed. Snelling, N.J., Blackwell Scientific Publications, Oxford.

Dodson, M.H., Dunn, J.R., Fuller, M., Williams, I., Ito, H., Schmidt, V.A., Wu, Yu.M., 1978. Palaeomagnetic record of a late Tertiary field reversal, *Geophys. J. R. astr. Soc.,* **53,** 373–412.

Dunlop, D.J., Özdemir, Ö., Clark, D.A. & Schmidt, P.W., 2000. Time-temperature relations for the remagnetization of pyrrhotite (Fe7S8) and their use in estimating paleo-temperatures, *Earth planet. Sci. Lett.,* **176,** 107–116.

Elmore, R.D. & McCabe, C., 1991. The occurrence and origin of remagnetization in the sedimentary rocks of North Americas, in *Contributions in Geomagnetism and Paleomagnetism, US Nat. Rept Int. Un. Geod. Geophys., 1987–1990, Rev. Geophys.,* **29,** 377–383.

Elmore, R.D., London, D., Bagley, D., Fruit, D. & Guoqiu, G., 1993. Remagnetization by basinal fluids: Testing the hypothesis in the Viola Limestone, southern Oklahoma, *J. geophys. Res.,* **98,** 6237–6254.

England, P., Le Fort, P., Molnar, P. & Pêcher, A., 1992. Heat sources for Tertiary metamorphism and anatexis in the Annapurna-Manaslu Region Central Nepal, *J. geophys Res.,* **97** (B2), 2107–2128.

Fuchs, G., 1967. Zum Bau des Himalaya, *Österreichische Akademie der Wissenschaften,* **113 band,** 1–212.

Fuchs, G., 1977. The geology of Karnali and Dolpo regions, western Nepal, *Jahrb. Geol. Bundesanstalt,* **120,** 165–217.

Fuchs, G., 1982. *Explanation of the Geologic Tectonic Map of the Himalaya,* Geol. Surv. Austria, Vienna.

Gansser, A., 1964. *Geology of the Himalayas,* J. Wiley, New York.

Gansser, A., 1981. The geodynamic history of the Himalaya, *AGU Geodyn. Ser.,* **3,** 111–121.

Garzanti, E. & Pagni Frette, M., 1991. Stratigraphic succession of the Thakkhola region (Central Nepal): comparison with the Northwestern Tethys Himalaya, *Rivista Italiana Di Paleontologia E Stratigrafia,* **97,** 3–26.

Garzanti, E., Gorza, M., Martellini, L. & Nicora, A., 1994. Transition from diagenesis to metamorphism in the Paleozoic to Mesozoic succession of the Dolpo-Manang synclinorium and Thakkola Graben (Nepal Tethys Himalaya), *Eclog. Geol. Helv.,* **87,** 613–632.

Godin, L., Brown, R.L. & Hanmer, S., 1999a. High strain zone in hanging wall of the Annapurna Detachment, central Nepal Himalaya, in *Himalaya and Tibet: Mountain Roots to Mountain Tops,* eds Macfarlane, A., Sorkhabi, R. & Quade, J, *Geol. Soc. Am. Spec. Pap.,* **328,** 199–210.

Godin, L., Brown, R.L., Hanmer, S. & Parrish, R., 1999b. Back folds in the core of the Himalayan orogen: an alternative interpretation, *Geology,* **27,** 151–154.

Guillot, S., Cosca, M., Allemand, P. & Le Fort, P., 1999. Contrasting metamorphic and geochronologic evolution along the Himalayan belt, in *Himalaya and Tibet: Mountain Roots to Mountain Tops,* eds Macfarlane, A., Sorkhabi, R. & Quade, J., *Geol. Soc. Am. Spec. Pap.,* **328,** 117–128.

Hrouda, F., 1994. A technique for the measurement of thermal changes of magnetic susceptibility of weakly magnetic rocks by the CS-apparatus and KLY-2 Kappabridge, *Geophys. J. Int.,* **118,** 604–612.

Katz, B., Elmore, R.D., Cogoini, M., Engel, M.H. & Ferry, S., 2000. Associations between burial diagenesis of smectite, chemical remagnetization, and magnetite authigenesis in the Vocontian trough, SE France, *J. geophys Res.,* **105** (B1), 851–868.

Kirschvink, J.L., 1980. The least-square line and plane and the analysis of paleomagnetic data, *Geophys. J. R. astr. Soc.,* **62,** 699–718.

Le Fort, P., 1986. The 500 Ma magmatic event in Alpine Southern Asia episode at Gondwana scale, *Mém. Sci. Terre, Nancy,* **47,** 191–209.

Le Fort, P. & France Lanord, C., 1995. Granites from Mustang and surrounding regions (Central Nepal), *J. Nepal Geol. Soc.,* **11,** 53–58.

McCabe, C., Jackson, M. & Saffe, R.B., 1989. Regional patterns of magnetite authigenesis in the Appalachian Basin; implications for the mechanism of late Paleozoïc remagnetization, *J. geophys Res.,* **94,** 10 429–10 443.

McElhinny, M.W., 1964. Statistical significance of fold test in paleomagnetism, *Geophys. J. R. astr. Soc.,* **8,** 338–340.

Ménard, G. & Rochette, P., 1992. Utilisation de réaimantation postmétamorphique pour une étude de l'évolution tectonique et thermique tardive dans les Alpes occidentales (France), *Bull. Soc. Géol. France,* **163,** 381–392.

Néel, L., 1949. Théorie du trainage magnétique des ferromagnétiques en grains fins avec applications aux terres cuites, *Ann. Géophys.,* **5,** 99–136.

Pan, H., Symons, D.T.A. & Sangster, D.F., 1990. Paleomagnetism of the Mississipi Valley type ores and host rocks in the northern Arkansas and Tri-State Districts, *Can. J. Earth Sci.,* **27,** 923–931.

Piper, J.D.A., 1981. The altitude dependence of magnetic remanence in the slowly-cooled Precambrian plutonic terrain of Western Greenland, *Earth planet. Sci. Lett.,* **54,** 449–466.

Pullaiah, G., Irving, E., Buchan, K.L. & Dunlop, D.J., 1975. Magnetization changes caused by burial and uplift, *Earth Planet. Sci. Lett.,* **28,** 133–143.

Ratschbacher, L., Frisch, W. & Guanghua, L., 1994. Distributed deformation in southern and western Tibet during and after the India-Asia collision, *J. geophys. Res.,* **99,** 19 917–19 945.

Rochette, P., Ménard, G. & Dunn, R., 1992. Thermochronometry and cooling rates deduced from single sample records of successive magnetic polarities during uplift of metamorphic rocks in the Alps (France), *Geophys. J. Int.,* **108,** 491–501.

Rochette, P., Scaillet, S., Guillot, S., Le Fort, P. & Pêcher, A., 1994. Magnetic properties of the High Himalayan leucogranites: structural implications, *Earth planet. Sci. Lett.,* **126,** 214–234.

Schneider, C. & Masch, L., 1993. The metamorphism of the Tibetan Series from the Manang area Marsyangdi Valley, Central Nepal, in *Himalayan Tectonics,* eds Treloar, P.J. & Searle, M.P, *Geol. Soc. Lond. Spec. Publ.,* **74,** 357–374.

Vannay, J.C. & Hodges, K.V., 1996. Tectonometamorphic evolution of the Himalayan metamorphic core between the Annapurna and Dhaulagiri, central Nepal, *J. met. Geol.,* **14,** 635–656.

Wiesmayr, G. & Grasemann, B., 1999. Balanced cross-section and depth to detachment calculations for the Tethyan Himalaya (Spiti, N India): where is the crystalline basement of the Higher Himalaya? 14th HKTW, *Terra Nostra,* **2,** 172–173.

Williams, I. & Fuller, M., 1982. A Miocene polarity transition (R–N) from the Agno batholith Luzon, *J. geophys. Res.,* **87,** 9408–9418.